# Quadruped Robot Running With a Bounding Gait

S. Talebi[1]      I. Poulakakis[1]      E. Papadopoulos[2]      M. Buehler[1]

[1]Ambulatory Robotics Laboratory, http://www.mcgill.cim.ca/~arlweb
Centre for Intelligent Machines, McGill University, Montreal, CANADA
[2]Department of Mechanical Engineering, NTU Athens, GREECE

**Abstract:** Scout II, an autonomous four-legged robot with only one actuator per compliant leg is described. We demonstrate the need to model the actuators and the power source of the robot system carefully in order to obtain experimentally valid models for simulation and analysis. We describe a new, simple running controller that requires minimal task level feedback, yet achieves reliable and fast running up to 1.2 m/s. These results contribute to the increasing evidence that apparently complex dynamically dexterous tasks may be controlled via simple control laws. An energetics analysis reveals a highly efficient system with a specific resistance of 0.32 when based on mechanical power dissipation and of 1.0 when based on total electrical power dissipation.

## 1. Introduction

Most existing four- or eight-legged robots are designed for statically stable operation - stability is assured by keeping the machine's center of mass above the polygon formed by the supporting feet. While this is the safest mode of locomotion, it comes at the cost of mobility and speed. Furthermore it requires a high mechanical complexity of three degrees of freedom per leg to provide continuous body support.

In contrast, we have pursued an agenda of low mechanical complexity in our Scout I and II robots, in order to decrease cost and increase reliability. We have shown in [1, 2] that dynamic walking, turning and step climbing can be achieved with a quadruped with stiff legs and only one hip actuator per leg. In this paper we show that Scout II with an additional compliant prismatic joint per leg is able to bound (Fig. 1). Dynamic running is possible with a very simple control strategy. Open loop control, simply positioning the legs at a fixed angle during flight, and commanding a fixed leg sweep angular velocity during stance results in a stable bounding gait. To our knowledge, Scout II is the first autonomous quadruped that achieves compliant running, features the simplest running control algorithm, and the simplest mechanical design to date.

This paper also addresses two subjects that have not yet received the attention they require in order to advance the state of the art in autonomous, dynamically stable legged locomotion - experimentally validated models and
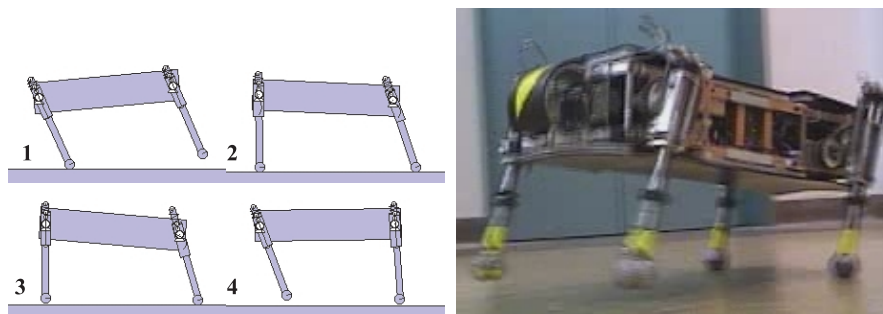
Figure 1. Illustration of a bound gait (left) and Scout II bounding (right)

energetics. Autonomous legged robots operate at the limits of their actuators, and require a model of the actuator dynamics and their interaction with the power source. We show that for Scout II, and likely for most other robots in its class, ignoring these issues results in inaccurate models. In addition, energy efficiency and autonomy are essential for mobile robots. In order to characterize the energetics of Scout II, we document the running efficiency as a function of speed, based on both the mechanical actuator output power, and the total electrical input power.

Ongoing research addresses compliant walking, rough terrain locomotion and dynamic stair climbing with Scout II, while another paper [3] demonstrated a trotting (walking) gait, based on additional passive, but lockable knee joints and non-compliant legs. The approach of using only one actuated degree of freedom per leg, compliant legs, and task-space open loop controllers has recently also been applied successfully to a dynamic hexaped, RHex [4]. This biologically inspired robot has the added advantage of a low center of mass and sprawled posture and is able to negotiate rough terrain at one body length per second.

Only few cases of quadruped running robots have been reported in the literature. About 15 years ago, Raibert [5] set the stage with his groundbreaking work on a dynamically stable quadruped, which implemented his three-part controller, via generalizations of the virtual leg idea. The robot featured three hydraulically actuated and one passive prismatic DOF per leg. The robot was able to trot, pace and bound, with smooth transitions between these gaits. Furusho et al [6] implemented a bounding gait on the Scamper robot. Even though the robot's legs were not designed with explicit mechanical compliance, the compliance of the feet, legs, belt transmissions, and the PD joint servo loops were likely significant. Akiyama and Kimura [7] implemented a bounding gait in the Patrush robot. Each three DOF leg featured an actuated hip and knee, and an unactuated, compliant foot joint. Their neural oscillator based controller was motivated by Matsuoka [8], which also underlies the control of the simulated planar biped of Taga et al [9]. An additional reflex network was added to the neural oscillator to achieve the stability and robustness necessary for experimental success.

## 2. Mechanical Structure and Modeling

The mechanical design of Scout II (Fig. 2) is an exercise in simplicity. Besides its modular design, the most striking feature is the fact that it uses a single actuator per leg - the hip joint provides leg rotation in the sagittal plane. Each leg assembly consists of a lower and an upper leg, connected via a spring to form a compliant prismatic joint. Thus each leg has two degrees of freedom, one actuated hip and one unactuated linear spring. All components for autonomous operation are integrated: The two hip assemblies contain the actuators and batteries, and the body houses all computing, interfacing and power distribution.
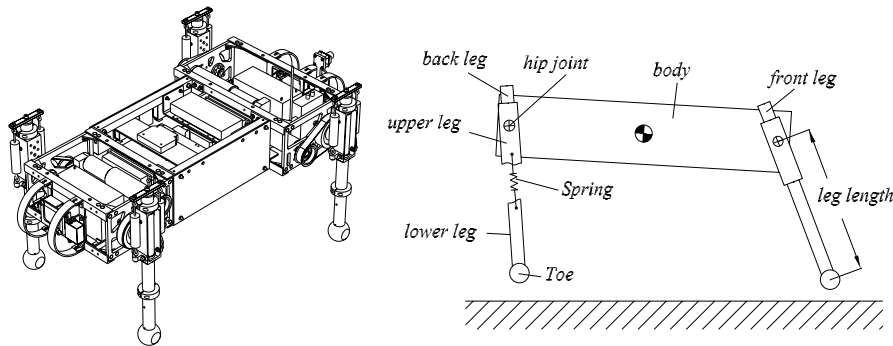


Figure 2. Scout II

The Scout II in planar motion is modeled in WorkingModel 2D [10] as a five-body kinematic chain, shown in Fig. 2. A linear spring and damper system models the leg compliance during stance phase. Since each of the two legs can be in stance or flight, there are four robot states.

## 3. Actuator and Power Source Modeling

It is well known that dynamically stable legged robots are complex dynamical systems with intermittent variable structure dynamics, fewer actuators than motion degrees of freedom, impacts, unilateral toe-ground constraints, and limited ability to apply tangential ground forces due to slip. These qualities greatly complicate modeling and usually prevent the application of classical control synthesis. In this section we demonstrate two additional modeling components which are dominant on our Scout II robot, and which are likely to be significant in dynamically stable legged robots in general - actuator and power source modeling.

Designing an autonomous dynamically stable robot is a formidable system design challenge. For example, the robot weight should be kept to a minimum, yet the actuators have to be capable not only to support the robot weight, but also to impart significant accelerations to the body, and support large dynamic loads. As a result, the actuators will typically operate at their limits, characterized by their torque-speed curve. While this fact is well known, it is typically not taken into account in robot modeling and control. As we will see below,

ignoring this constraint will result in large differences between commanded and actually achieved torques.

The torque speed limitation of an electrical actuator can be characterized in the first quadrant by

$$\tau = min(\frac{K}{R}(V_T - K\omega), \tau_{max}) \tag{1}$$

where K is the motor torque constant, R is the motor armature resistance, $\omega$ is the motor speed, $V_T$ is the motor terminal voltage, and $\tau_{max}$ is the fixed torque limit imposed by the motor amplifiers' current constraint. Figure 3 below shows the large difference between desired torques (top plots), and actually achievable torques (lower plots), for a fixed power supply or battery voltage.
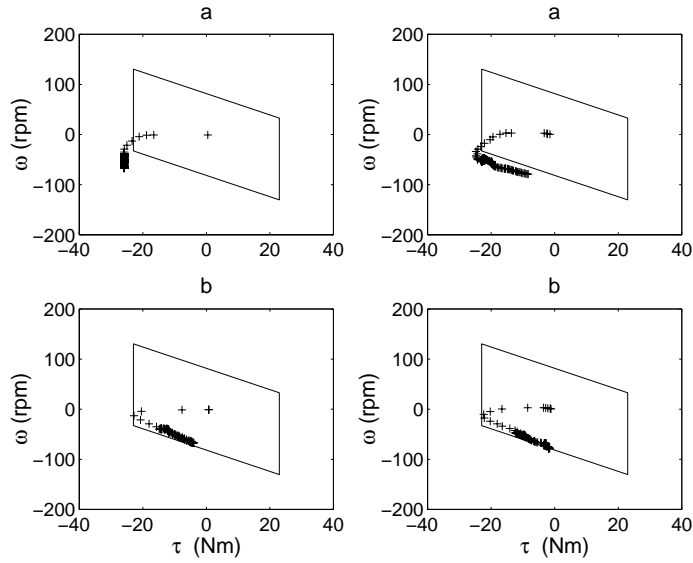


Figure 3. Experimental results. Torque speed plot for the back (left), and front legs (right) actuators. Top plot shows commanded torques and bottom plots show actually achievable torques, based on a fixed 24 V battery voltage (solid polygon).

Since electrically actuated autonomous robots can draw significant peak power and operate from non-ideal voltage sources, the variation of the supply voltage as a function of the total load current must be considered. Fig. 4 (left) shows the drastic supply voltage fluctuations, and that a simple battery model, consisting of a fixed internal voltage source of 24 V in series with an internal resistance of 0.15 $\Omega$ results in a very good match between the measured and modeled supply voltage.

Fig. 4 (right) demonstrates both the large discrepancy between desired (upper solid line) and achievable motor torques (lower solid line) and the accuracy of the combined actuator/power model. It is interesting to point out

that, due to the multitude of dynamic, actuation, and power constraints, it is
nearly impossible to control either torque or leg angular velocity during stance
arbitrarily. The controller can only affect the system dynamics during stance
in a limited fashion. For this reason it is important that the robot's passive
(unforced) dynamics be as close as possible to the desired motion. Indeed, this
is likely one of the reasons for the successful operation of Scout II. In addition,
the actuation constraints during stance suggest the use of the leg touchdown
angle (which is easily controlled during flight) as a dominant control input. As
shown in the following section, this is one of the main control parameter in our
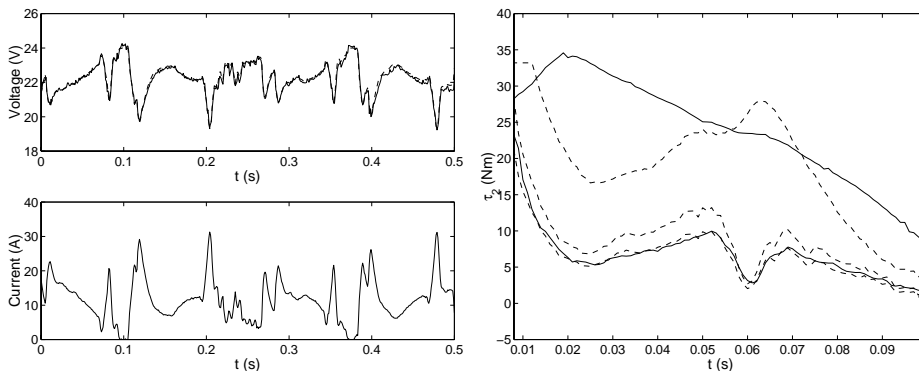bounding controller.



Figure 4. (left) Battery voltage fluctuation (top, solid) as a function of load cur-
rent (bottom). The top graph shows both the measured battery voltage (solid)
and the battery voltage estimation (dash). The exceptionally good match be-
tween experimental and model data validates the simple internal resistance
model (24V nom. battery voltage with 0.15 Ω internal resistance). Figure
4. (right) Torque profiles during one stance phase from touchdown until the
sweeplimit is reached. Data traces from top to bottom: Desired torque from
controller (solid), maximum achievable torque based on torque speed curve
with fixed 24 V supply voltage (dashed), max. achievable torque based on
battery voltage model; additional loop gain fix due to amplifier gain modeling
error; measured motor torque (solid).

## 4. Bounding Controller

Even though Scout II is an under-actuated, highly nonlinear, intermittent dy-
namical system, we found that simple a control laws can stabilize periodic
motions, resulting in robust and fast running. Surprisingly, the controllers do
not require task level feedback like forward velocity, or body angle. What is
more, there seem to exist many such simple stabilizing controllers - in [11] three
variations are introduced. It is remarkable that the significant controller differ-
ences have relatively minor effects on bounding performance! For this reason
and for brevity we shall describe one of these controllers here.

The controller is based on two individual, independent leg controllers,

without a notion of overall body state. The front and back legs each detect two leg states - stance (touching ground) and flight (otherwise), which are separated by touchdown and lift-off events.

There is no actively controlled coupling between the fore and hind legs - the resulting bounding motion is purely the result of the controller interaction through the multi-body dynamic system. During flight, the controller servos the flight leg to a desired touchdown angle $\phi_{td}$, then sweeps the leg during stance with a desired angular velocity $\dot{\phi}_d$ until a sweep limit $\phi_{sl}$ is reached. Table 1 lists these controller parameters and the stance and flight PD gains. Even though we show only the results for one of several controllers implemented, experimental performance for all of them is very similar - resulting in stable and robust bounding, at top speeds between 0.9 and 1.2 m/s.

|  | front and back legs |
|---|---|
| $\phi_{td}(^o)$ | 20 |
| $\phi_{sl}(^o)$ | 0 |
| $\dot{\phi}_d(^o/s)$ | -200 |
| $k_{p,s}$ & $k_{p,f}$ (Nm/ $^o$) | 35 |
| $k_{d,s}$ & $k_{d,f}$ (Nm/ $^o$) | 0.15 |

Table 1. Controller Parameters and PD gains (average speed 0.7m/s).

Figure 5 compares the body angle trajectories and torque profiles between simulations and experiment. The stride frequency as well as the body oscillation amplitude matches well. The torque traces are qualitatively similar, but there are still many details which differ. Some of these are likely due to inaccurately modeled ground-toe friction, and unmodeled compliance in the leg. These differences are still the subject of ongoing work.

## 5. Energetics

For mobile robots to be of practical utility, they need to be energy efficient and able to operate in a power-autonomous fashion for extended periods of time. Thus, energy efficiency is an important performance measure of mobile robots. An increasingly accepted measure of energy efficiency is the 'specific resistance' - a measure proposed originally by Gabrielli and von Kármán [12] in 1950,

$$\varepsilon(\nu) = \frac{P(\nu)}{mg\nu} \tag{2}$$

where $P$ is the power expenditure, $m$ is the mass of the vehicle, $g$ is the gravitational acceleration, and $\nu$ is the vehicle speed. Since many vehicle specific resistances quoted in the literature are based on the average mechanical output power of the actuators, we have calculated this figure as a function of speed (Fig. 6). Even though energy efficiency has so far not been optimized, Scout II at top speed already achieves a low specific resistance of $\varepsilon = 0.32$. This value places Scout II among the most energy efficient running robots, only slightly higher than the (lowest published running robot efficiency) $\varepsilon = 0.22$ value for the ARL Monopod II [13, 14], but still lower than any other running robot.
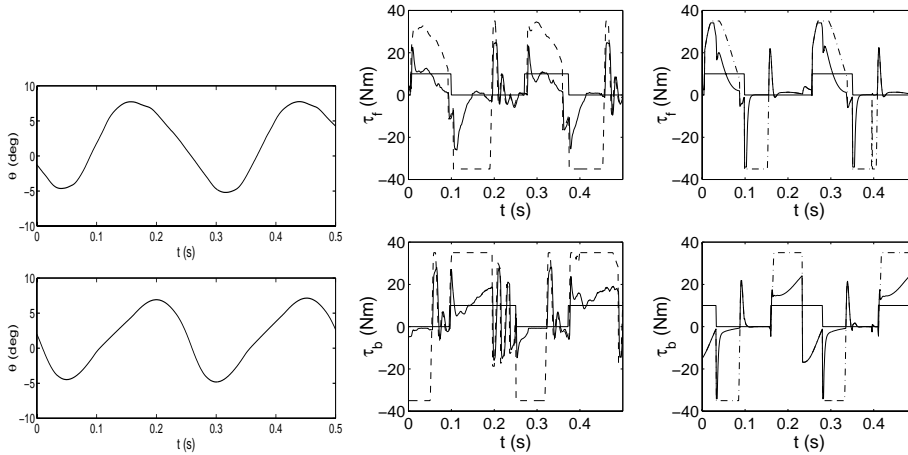
Figure 5. (left) Body angle . Experiment (top), simulation (bottom). Figure 5 (right) Front (top) and back (bottom) actuator torques. Commanded torques(dash) vs. measured torques (solid). Experiments (left) vs. simulation(right). The solid square wave denotes the leg state: stance (high)and flight (low).
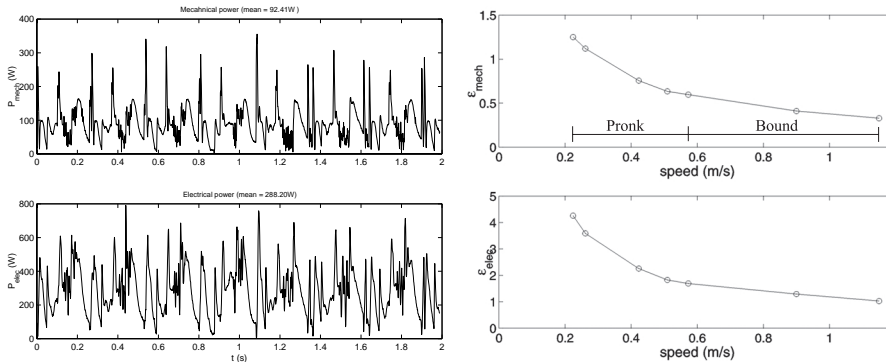


Figure 6. (left) Mechanical (top) and total electrical (bottom) power consumption at 1.15 m/s. Figure 6. (right) Specific resistance as a function of forward speed based on mechanical (top) and total electrical (bottom) power consumption.

The specific resistance based on mechanical output power has drawbacks, since it does not take the actuator efficiency or the power consumption of the entire system into account. Both of these effects can have a dramatic negative influence on runtime. Therefore, a more useful measure of energy efficiency, is the specific resistance based on total power consumption. For a system with a battery as the main power source, this is the total average product of battery current and voltage. For Scout II, this value is approximately $\varepsilon = 1.0$, three times the specific resistance based on mechanical power. We suspect that

this value is still low for a running robot, and that even the large difference between electrical and mechanical power is normal; however, little comparable data is available from other robots to date, and we hope that the reporting of mechanical output power and total electrical input power will become standard practice for mobile robots in the future.

## 6. Conclusion

In this paper we have presented an algorithm that controls compliant bounding for a quadruped robot with only one actuator per leg. The algorithm was derived and tested in simulations, which incorporated a validated model for the actuators and the power source. Experimental runs showed good correspondence with the simulations. Experimental data was used to show a low specific resistance of $\varepsilon = 0.32$ when based on mechanical power and of $\varepsilon = 1.0$ when based on total electrical power.

## 7. Acknowledgements

## References

[1] M. Buehler, R. Battaglia, A. Cocosco, G. Hawker, J. Sarkis, and K. Yamazaki. Scout: A simple quadruped that walks, climbs and runs. In *IEEE Int. Conf. Robotics and Automation*, pages 1707–1712, May 1998.

[2] M. Buehler, A. Cocosco, K. Yamazaki, and R. Battaglia. Stable open loop walking in quadruped robots with stick legs. In *IEEE Int. Conf. Robotics and Automation*, pages 2348–2353, May 1999.

[3] G. Hawker and M. Buehler. Quadruped trotting with passive knees. In *IEEE Int. Conf. Robotics and Automation*, pages 3046–3051, April 2000.

[4] U. Saranli, M. Buehler, and D. E. Koditchek. Design, modelling and preliminary control of a compliant hexapod robot. In *IEEE Int. Conf. Robotics and Automation*, pages 2589–2596, April 2000.

[5] M. H. Raibert. *Legged Robots that Balance*. MIT Press, Cambridge, MA, 1986.

[6] J. Furusho, A. Sano, M. Sakaguchi, and E. Koizumi. Realization of bounce gait in a quadruped robot with articular-joint-type legs. In *IEEE Int. Conf. Robotics and Automation*, pages 697–702, May 1995.

[7] S. Akiyama and H. Kimura. Dynamic quadruped walk using neural oscillators - realization of pace and trot. In *13. Annual Conf. RSJ*, pages 227–228, 1995.

[8] K. Matsuoka. Sustained oscillations generated by mutually inhibiting neurons with adaptation. *Biol. Cybernetics*, 52:367–376, 1985.

[9] G. Taga, Y. Yamaguchi, and H. Shimizu. Self-organized control of bipedal locomotion by neural oscillators in unpredictable environment. *Biol. Cybernetics*, 65:147–159, 1991.

[10] Knowledge Revolution. *Working Model 2D User's Guide*. CA, 1996.

[11] S. Talebi. Compliant running and step climbing of the Scout II platform. Master's thesis, McGill University, 2000.

[12] G. Gabrielli and Th. von Kármán. What price speed? *Mechanical Engineering*, 72(10):775–781, 1950.

[13] M. Ahmadi and M. Buehler. The ARL Monopod II running robot: Control and energetics. In *IEEE Int. Conf. Robotics and Automation*, pages 1689–1694, May 1999.

[14] M. Ahmadi and M. Buehler. Stable control of a simulated one-legged running robot with hip and leg compliance. *IEEE Trans. Robotics and Automation*, pages 96–104, Feb 1997.